



# Entanglement production in the Sachdev–Ye–Kitaev Model and its variants

Tanay Pathak <sup>1,2,\*</sup> and Masaki Tezuka <sup>2,†</sup>

<sup>1</sup>*Center for Gravitational Physics and Quantum Information, Yukawa Institute for Theoretical Physics, Kyoto University, Kitashirakawa Oiwakecho, Sakyo-ku, Kyoto 606-8502, Japan*

<sup>2</sup>*Department of Physics, Kyoto University, Kitashirakawa Oiwakecho, Sakyo-ku, Kyoto 606-8502, Japan*

Understanding how quantum chaotic systems generate entanglement can provide insight into their microscopic chaotic dynamics and can help distinguish between different classes of chaotic behavior. Using von Neumann entanglement entropy, we study a nonentangled state evolved under three variants of the Sachdev–Ye–Kitaev (SYK) model with a finite number of Majorana fermions  $N$ . All the variants exhibit linear entanglement growth at early times, which at late times saturates to a universal value consistent with random matrix theory (RMT), but their growth rates differ. We interpret this as a large- $N$  effect, arising from the enhanced non-locality of fermionic operators in SYK and binary SYK, absent in spin operators of the spin-SYK model. Numerically, we find that these differences emerge gradually with increasing  $N$ . Although all variants are quantum chaotic, their entanglement dynamics reflect varying degrees of chaos and indicate that the entanglement production rate serves as a fine-grained probe of chaos beyond conventional measures. To probe its effect on thermalization properties of these models, we study the two-point autocorrelation function, finding no differences between the SYK variants, but deviations from RMT predictions for  $N \geq 24$ , particularly near the crossover from exponential decay to saturation regime.

*Introduction:* The Sachdev–Ye–Kitaev (SYK) model is a model of  $N$  fermions with  $q$ -body all-to-all random interactions [1–3]. Given its simplicity along with rich physics, it has emerged as a paradigmatic model of quantum chaos and holography recently [4–14]. There are proposals to realize it experimentally such as using Rydberg atoms as quantum simulators for the SYK model [15] or recently the possibility to observe SYK physics at low temperature and in high magnetic field using graphene quantum dots [16]. There are other proposed realization of the model such as in quantum computer simulations [17–23]. Efforts have been made to further simplify the model for a more feasible experimental realization. Variants of interest are the sparse SYK model [24–30] and the spin SYK model [31, 32]. Various other variants have been studied in the literature for their interesting properties in high energy as well as condensed matter physics [33–60].

In this paper, we focus on three variants: the sparse SYK model, the binary sparse SYK model and the sparse spin SYK model. For deciding whether they are suitable targets for practical implementation, a natural question to ask is: *To what extent are these models similar(different) to(from) each other?* Some comparisons based on information recovery and finite- $N$  spectrum of these variants had been carried out in [30, 32, 61, 62]. In this work we attempt the first systematic effort to quantitatively compare the SYK, sparse variants of SYK, and RMT for their (dynamical) chaotic properties using the entanglement production process. The results presented here thus also serve as a sensitive test to compare the result of SYK model with corresponding random matrices. The entanglement entropy has already been well studied for its relationship with quantum chaos

[63–71]. It has also been observed that given a less entangled(unentangled) state evolving under the action of a given quantum chaotic Hamiltonian, its entanglement is substantially enhanced [72–81]. For strongly chaotic system the entanglement production saturates at late times [66, 75] which is a statistical property and based on random matrix theory (RMT) modeling a statistical bound on entanglement entropy was proposed in [82]. The entanglement production can thus be used as a criterion of dynamical chaos in quantum chaotic systems [83–85]. We use the entanglement production rate as a metric to compare the three variants of the SYK models and quantify their chaotic nature.

*Random Matrix Theory:* We briefly recapitulate the bound on the entanglement entropy based on random matrix theory modeling as discussed in [75, 82] for completeness. Consider a bi-partition of the Hilbert space,  $\mathcal{H} = \mathcal{H}_A \otimes \mathcal{H}_B$  of dimension  $\mathcal{D}$ . Without loss of generality we consider,  $\dim(\mathcal{H}_A) = \mathcal{N} \leq \dim(\mathcal{H}_B) = \mathcal{M}$ ,  $\mathcal{D} = \mathcal{N} \times \mathcal{M}$ . The reduced density matrix constructed from an eigenstate of random matrices (by tracing out, say system  $B$ ) belong to ensemble of trace restricted Wishart matrices [75, 82];  $\rho_{A,B} = \frac{G^\dagger G}{\text{Tr}(G^\dagger G)}$ , where  $G$  is an unstructured  $\mathcal{N} \times \mathcal{N}$  Gaussian random matrix. The average density of states of ensemble of Wishart matrices is given by the Marchenko–Pastur distribution [86] and using it a bound on the average entanglement entropy was proposed in [82], which can be compactly written as [87] (see also [88]), as follows

$$\langle S_E \rangle \cong \ln(\mathcal{N}) - \frac{1}{2Q}; \quad Q = \frac{\mathcal{M}}{\mathcal{N}} \quad (1)$$

which corresponds to Page’s result for the average EE of a random pure state, for  $1 \ll \mathcal{N} < \mathcal{M}$  [89, 90]. If we now

start with an initial state and let it evolve in time using a quantum chaotic Hamiltonian then at late times the EE will saturate the statistical bound, Eq.(1). For the extreme case where the initial state is a product state, the EE will be zero at the start and will eventually grow to saturate the bound at late times. For the other case where the initial state is a maximally entangled state, for which the EE is already maximal (and also greater than the above bound), the evolution in time will lead to an initial *decrease* of EE which then ultimately saturates the bound at late times [82]. We verify these results numerically for the case of GOE and GUE matrices (see Supplemental material [88]).

*The models:* We mainly focus on the three variants of the SYK model which were proposed for their feasibility of simulation in quantum computers (see [91] for study in spin models). The SYK model preserves parity, therefore the Hamiltonian can be written in block diagonal form, with two blocks [7]. For each of these models, care is also taken to ensure that the variance of eigenvalues is the same (see Supplemental material for details on numerical methods [88]). This is important to ensure proper comparison of all the *relevant time scales* among the three models. Furthermore, the product state ( $\psi_P$ ) that we consider throughout the paper is [92]

$$\Psi_P = \bigotimes_{i=1}^n \frac{1}{\sqrt{2}}(|0\rangle + |1\rangle). \quad (2)$$

1. *The sparse SYK model:* We start with the usual SYK model [4] which is a model of  $q$ -fermion interactions whose Hamiltonian is given by

$$H = \sqrt{\frac{(q-1)!}{N^{q-1}}} \sum_{1 \leq i_1 < \dots < i_q \leq N} J_{i_1 i_2 \dots i_q} \psi_{i_1} \psi_{i_2} \dots \psi_{i_q}, \quad (3)$$

where  $\psi_i$  are the Fermionic operators which satisfy the Clifford algebra:  $\{\psi_i, \psi_j\} = \delta_{ij}$  and  $J_{i_1 i_2 \dots i_q}$  are standard Gaussian random variables with probability distribution function  $P(J_{i_1 \dots i_q}) = \frac{1}{\sqrt{2\pi}} e^{-J_{i_1 \dots i_q}^2/2}$ . We specialize to the  $q = 4$  case (SYK<sub>4</sub>, which we call SYK for brevity). Furthermore, we consider a simple generalization of the SYK model with the aim that the features of Hamiltonian given by Eq. (4) remains intact and at the same time with lesser complexity is the sparse SYK model [24–29] which is defined as follows

$$H = \sqrt{\frac{6}{pN^3}} \sum_{1 \leq i < j < k < l \leq N} x_{ijkl} J_{ijkl} \psi_i \psi_j \psi_k \psi_l, \quad (4)$$

where  $x_{ijkl}$  is randomly chosen to be 1 or 0 with probability  $p$  and  $1-p$ , respectively, and  $J_{i_1 i_2 i_3 i_4}$  are standard Gaussian random variables. The model is then equivalent to the deletion of some terms in the dense SYK model Hamiltonian (implying no deletion of terms i.e.  $p = 1$ ).

2. *The Binary SYK model:* Another important variant

of the SYK model is binary sparse SYK model (SYK<sub>b</sub>) where the couplings of the model are nonzero with probability  $p$  and zero with probability  $1-p$ . The non-zero couplings are either  $+1$  and  $-1$  with probability  $p/2$  each. This model is a simplification of the original model, and as has been pointed out in [93] it is an improvement and matches with the RMT predictions better as compared to the corresponding sparse SYK model. For the numerical purpose, we follow [93] and keep the number of non-zero couplings as fixed,  $\kappa$ . The number of couplings  $J_{i_1 i_2 i_3 i_4}$  that take values  $\pm 1$ , is  $\kappa/2$  when  $\kappa$  is even, and  $(\kappa \pm 1)/2$  when  $\kappa$  is odd. The remaining,  $\binom{N}{4} - \kappa$ , couplings are 0. From this we can obtain  $p$  as  $p = \frac{\kappa}{\binom{N}{4}}$ . The Hamiltonian is given by

$$H = \sqrt{\frac{6}{pN^3}} \sum_{1 \leq i_1 < i_2 < i_3 < i_4 \leq N} J_{i_1 i_2 i_3 i_4} \psi_{i_1} \psi_{i_2} \psi_{i_3} \psi_{i_4}, \quad (5)$$

3. *The spin-SYK model:* The spin-SYK (SYK<sub>s</sub>) is a variant where the Majorana fermions in the SYK model are replaced by Pauli spin operators [32]. The spin analogue of fermionic operators,  $\hat{O}_a$ , are defined as:  $\hat{O}_{2j-1} = \hat{\sigma}_{j,x}$ ,  $\hat{O}_{2j} = \hat{\sigma}_{j,y}$ ;  $j = 1, 2, 3, \dots, N/2$ . Here,  $\sigma_{i,k} = \hat{I}_{i-1} \otimes \sigma_{i,k} \otimes \hat{I}_{N-i}$  and  $\hat{I}_l$  denotes the  $2^l$ -dimensional identity operator. Operators on the same spin anti-commute while operators on different spins commute. The sparse spin SYK Hamiltonian is then given as

$$H_s = \sqrt{\frac{6}{p(2N)^3}} \sum_{1 \leq i < j < k < l \leq 2N} x_{ijkl} J_{ijkl} i^{\eta_{ijkl}} \hat{O}_i \hat{O}_j \hat{O}_k \hat{O}_l, \quad (6)$$

where  $J_{ijkl}$  are standard Gaussian random variables,  $x_{ijkl}$  is 1 with probability  $p$  and 0 with probability  $1-p$ , similar to the case of the sparse SYK model.  $p = 1$  corresponds to the full dense spin SYK model.  $\eta_{ijkl}$  is the number of spins whose both  $x$  and  $y$  components appear in  $(i, j, k, l)$  and the factor  $i^{\eta_{ijkl}}$  ensures hermiticity of the Hamiltonian. Note that the variance of eigenvalues remains the same as in the previous two variants.

*Results: Entangling rate*—First we show the general observed behavior for the three variants for different degrees of sparseness in Fig. (1). For all the three variants we find an initial *linear* increase in entropy which then saturates at later time to a value given by Eq. (1). We further note that after a certain degree of sparseness, the entanglement production is not enough to saturate the bound. This critical value after which the entanglement entropy does not reach the bound (numerically checked till  $t = 30$  everywhere) is found to be:  $p_c = 0.004$  for SYK,  $\kappa_c = 22$  ( $p_c \approx 0.002$ ) for SYK<sub>b</sub> and  $p_c = 0.01$  for SYK<sub>s</sub>. This scenario can be attributed to the chaotic to integrable transition of the sparse SYK model and variants as the value of  $p$  ( $\kappa$ ) decreases (increase of sparsity) [26, 29, 30]. It is also to be noticed that the critical spar-

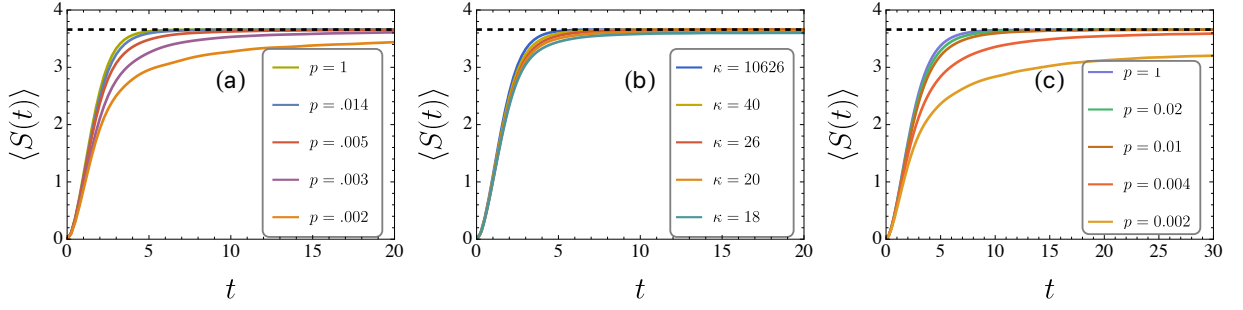


FIG. 1. (a), (b), (c) Evolution of EE of a product state with time, for SYK, binary SYK and the spin SYK model respectively. We do not resolve symmetry but it can be shown that the qualitative behavior remains the same (see [88] for further details on symmetry). The horizontal black line corresponds to the analytical result given by Eq. (1). We take  $N = 24$  for SYK and  $N = 12$  for  $\text{SYK}_s$ . Averaging is done over 50 realizations. The results are only shown for sparseness parameter values for which the different curves can be distinguished properly (see [88] for result of other intermediate values of sparse parameter  $p$  and  $\kappa$ ).

sity at which the breakdown occurs is lowest for  $\text{SYK}_b$  while it is highest for  $\text{SYK}_s$ .

Next, we contrast the behavior of the dense versions of the three variants and compare the entanglement production rate of these models with the GOE and GUE-type random matrices [88]. With initial product state, the entanglement entropy grows linearly and then saturates at the universal value as shown in Fig. 2. GOE and GUE type random matrices have the same rate while all the variants of the SYK model show deviations from the (Gaussian) random matrix behavior. Furthermore, SYK and  $\text{SYK}_b$  have the same slope in the linear growth regime that differs from the  $\text{SYK}_s$  model. Thus we find

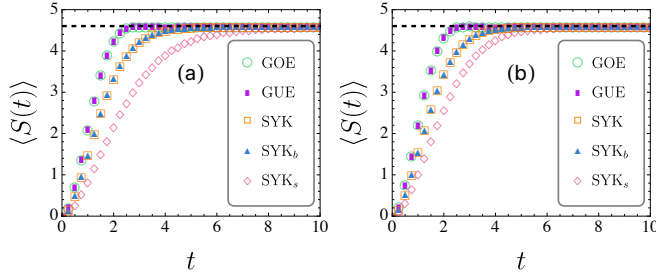


FIG. 2. (a) The evolution of the EE for initial product state using (dense;  $p = 1$ ) SYK and  $\text{SYK}_b$  with  $N = 30$  fermions (no symmetry resolution) and  $\text{SYK}_s$  with  $N = 15$  spins. Also shown are the results for random matrices of GOE and GUE type and dimensions  $2^{15}$ . We consider 50 realization of each of them. Slopes of best fit line in the linear regime (observed for  $t \geq 0.5$  for all the models) are—GOE:  $2.65 \pm 0.1$ , GUE:  $2.65 \pm 0.1$ , SYK:  $2.05 \pm 0.03$ ,  $\text{SYK}_b$ :  $2.05 \pm 0.03$ , and  $\text{SYK}_s$ :  $1.51 \pm 0.03$ . (b) Same as (a), but with SYK and  $\text{SYK}_b$  with  $N = 32$  fermions and  $\text{SYK}_s$  with  $N = 15$  spin, and considering only the odd parity block. Slopes of best fit line in the linear regime (observed for  $t \geq 0.5$  for all the models) are—GOE:  $2.60 \pm 0.08$ , GUE:  $2.60 \pm 0.08$ , SYK:  $1.99 \pm 0.02$ ,  $\text{SYK}_b$ :  $1.99 \pm 0.02$ ,  $\text{SYK}_s$ :  $1.26 \pm 0.03$ . In both cases, SYK models show systematic deviation from random matrix predictions.

that all the variants form a clear hierarchy based on their entangling rate:  $\text{SYK}_b \approx \text{SYK} > \text{SYK}_s$  and also show deviations from the (Gaussian) random matrix behavior. Note that if we take sparseness into account we find that the  $\text{SYK}_b$  retains these features for much smaller values of sparseness parameter  $p$  as compared to SYK and  $\text{SYK}_s$ . Based on the detailed numerical results pre-

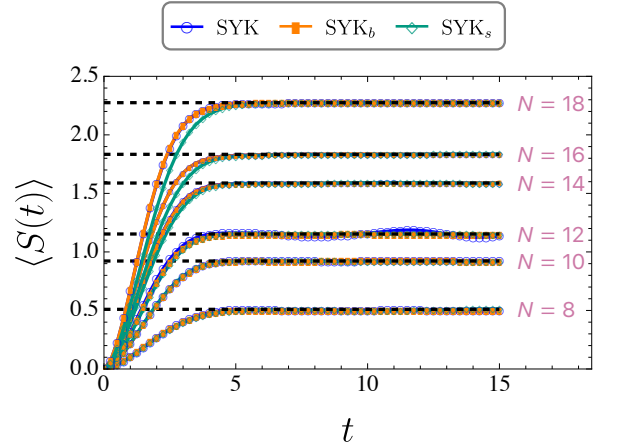


FIG. 3. Evolution of average EE of initial product state,  $\psi_p$ , for SYK model (spin resolved) with  $N=8(10^4)$ ,  $10(5000)$ ,  $12(2000)$ ,  $14(1000)$ ,  $16(500)$ ,  $18(250)$ , number of Majorana fermions (correspondingly we consider  $N/2$  spins for spin SYK), where values in the bracket denotes the number of Hamiltonian realization considered. EE is calculated by partially tracing out  $2^2$  dimensional subspace for  $N = 8, 10, 12$ ;  $2^3$  dimensional subspace for  $N = 14, 16$  and  $2^4$  dimensional subspace for  $N = 18$ . The dashed line denotes the thermal value [89] (we cannot directly use Eq. (1) as the subsystem sizes are too small for it to be valid). Observe the gradual deviations of the values for  $\text{SYK}_s$  as  $N$  increases.

sented here and previous studies on the SYK model and its variants we conclude that  $\text{SYK}_s$  is slightly less (dynamically) chaotic than the other two. The entanglement

under its action eventually reaches the thermal value, though slowly, suggesting different microscopic thermalization properties. The origin of this behavior can be attributed to the locality in  $\text{SYK}_s$  which is absent in the other two models once the Majorana operator and spin operators of the model are written as Pauli string [32]. To confirm this assertion, we study the effect of  $N$  on the evolution of EE for small values of  $N$  where the locality should not play a major role and hence all the models should behave in the same manner. As  $N$  increases SYK and  $\text{SYK}_b$  have more and more operators which have non-local Pauli strings, while  $\text{SYK}_s$  still has local strings. Hence, strictly speaking, the deviation of  $\text{SYK}_s$  results from SYK and  $\text{SYK}_b$  should be a large  $N$  effect and not observed for small  $N$ . In Fig. 3, we show the results for the entanglement production with initial product state and different values of  $N = 8, \dots, 18$ . As asserted, we observe there are no discernible differences between the three variants upto  $N = 12$ . From  $N = 14$ , entangling rate of  $\text{SYK}_s$  starts to deviate from the other two and the deviations become prominent as  $N$  increases further. This thus confirms our assertion.

*Two-point correlation function*—With the differences in the entangling rate it is thus natural to study its effects on the thermalization and operator growth properties of the model. As a first step towards studying thermalization properties we study two-point autocorrelation function for these model. Choosing the initial state as the product state,  $\psi_p$ , and Majorana operator  $\psi_1$ , we study the two-point autocorrelation  $\langle C(t) \rangle = \langle \langle \Psi_p | \psi_1(t) \psi_1 | \Psi_p \rangle \rangle$ , where  $\langle \cdot \rangle$  denotes the ensemble average over different Hamiltonian realizations. Considering the odd parity sector of the SYK Hamiltonian and the corresponding results are shown in Fig. (4). We observe that the autocorrelation function has the characteristics features that of chaotic systems: an *exponential* decay regime at early times and a saturation value at late times that decreases with  $N$  (see also [88] for supporting results). Though we do not find differences between the three variants, we observe slight deviations from RMT for  $N \geq 24$  near the transition from decay to saturation regime. These differences between RMT and the SYK model are observed to increase with value of  $N$ .

*Conclusions:* In this work we study the entanglement production of an initial product state using the SYK model, binary SYK ( $\text{SYK}_b$ ) and spin SYK ( $\text{SYK}_s$ ). The  $\text{SYK}_s$  model shows slower entanglement growth rate than the other two which show identical behavior. We assert that this behavior is due to the local structure in the spin SYK model and numerically confirm this for small  $N$  where this effect would not be significant. We also remark that, although eigenvalue correlation features of all these models closely follow the RMT prediction (with small deviations near the tail for the spin-SYK), their entanglement production rates do not match the RMT behavior (strictly speaking, the Gaussian RMT behav-

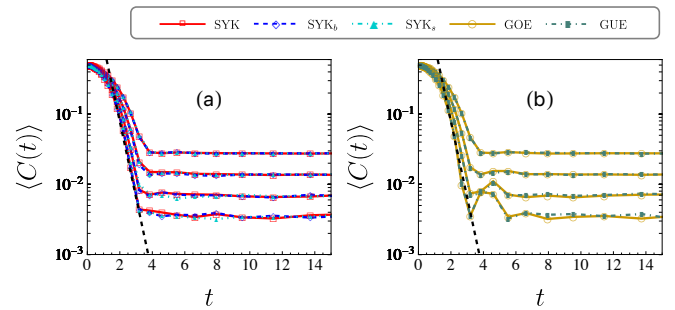


FIG. 4. (a) Autocorrelation function for Majorana operator  $\hat{O} = \psi_1$ , for different kinds of SYK model. The overlapping legends are for SYK,  $\text{SYK}_b$  and  $\text{SYK}_s$  for  $N = 18(5000), 22(1000), 26(200), 30(100)$  of Majorana fermions (and  $N/2$  number of spins for  $\text{SYK}_s$ ). The number in the bracket denotes the number of Hamiltonian realizations. We only consider odd parity sector. (b) Autocorrelation function for corresponding random matrices of GOE and GUE type of dimensions  $2^{N/2-1}$ . Black dashed curve represent the best fit curve;  $ae^{-bx}$ ;  $b = 2.49 \pm 0.23$ , in the exponential decay regime obtained using the data for  $2^{14}$  dimensional random matrices.

ior). SYK and  $\text{SYK}_b$  are closest to the RMT values but still show deviations, at least for the finite size systems considered. These results are some of the only differences from RMT found for the SYK model. The entanglement production rate can therefore serve as a sensitive probe highlighting differences between physical models and their associated RMT ensemble that ignore the fine-grained details of these models. To study its effect on thermalization properties we also studied the autocorrelation function. We find good agreement in the decay and saturation regimes, with small differences only near the transition regime and large  $N (\geq 24)$ .

It is important to note that in holographic theories the butterfly velocity ( $v_B$ ) that governs the rate of the growth of an operator under chaotic dynamics is related to the entanglement velocity ( $v_E$ ), i.e. the rate at which the entanglement spreads [94–97] as  $v_E \leq v_B$ . This further links the entangling rate to the properties of operator growth in the systems. Since locality played a major role in the entanglement production it will also be interesting to study other variants of the SYK model such as the recently introduced two-local modification [98] within this framework.

*Acknowledgments:* Numerical computations were performed using the computational facilities of the Yukawa Institute for Theoretical Physics. TP acknowledges the partial support of the Yukawa Research Fellowship, supported by the Yukawa Memorial Foundation and JST CREST (Grant No. JPMJCR19T2). The work was partially supported by JST CREST (Grant No. JPMJCR24I2). M. T. was partially supported by the Japan Society for the Promotion of Science (JSPS) Grants-

in-Aid for Scientific Research (KAKENHI) Grants No. JP21H05185 and JP25K00925.

- 
- \* [pathak.tanay.4s@kyoto-u.ac.jp](mailto:pathak.tanay.4s@kyoto-u.ac.jp)  
† [tezuka@scphys.kyoto-u.ac.jp](mailto:tezuka@scphys.kyoto-u.ac.jp)
- [1] S. Sachdev and J. Ye, Gapless spin-fluid ground state in a random quantum Heisenberg magnet, *Phys. Rev. Lett.* **70**, 3339 (1993).
  - [2] A. Kitaev, Hidden correlations in the Hawking radiation and thermal noise, talk at KITP, 2015 (2015).
  - [3] A. Kitaev, A simple model of quantum holography, Talks at KITP (2015), available online: <http://online.kitp.ucsb.edu/online/entangled15/kitaev/> and <http://online.kitp.ucsb.edu/online/entangled15/kitaev2/>.
  - [4] J. Maldacena and D. Stanford, Remarks on the Sachdev-Ye-Kitaev model, *Phys. Rev. D* **94**, 106002 (2016), [arXiv:1604.07818](https://arxiv.org/abs/1604.07818) [hep-th].
  - [5] A. M. García-García and J. J. M. Verbaarschot, Spectral and thermodynamic properties of the Sachdev-Ye-Kitaev model, *Phys. Rev. D* **94**, 126010 (2016), [arXiv:1610.03816](https://arxiv.org/abs/1610.03816) [hep-th].
  - [6] J. S. Cotler, G. Gur-Ari, M. Hanada, J. Polchinski, P. Saad, S. H. Shenker, D. Stanford, A. Streicher, and M. Tezuka, Black Holes and Random Matrices, *JHEP* **05**, 118, [Erratum: *JHEP* 09, 002 (2018)], [arXiv:1611.04650](https://arxiv.org/abs/1611.04650) [hep-th].
  - [7] C. Krishnan, K. V. Pavan Kumar, and D. Rosa, Contrasting SYK-like models, *Journal of High Energy Physics* **2018**, 10.1007/jhep01(2018)064 (2018).
  - [8] G. Sarosi, AdS<sub>2</sub> holography and the SYK model, in *Proceedings of XIII Modave Summer School in Mathematical Physics — PoS(Modave2017)*, Modave2017 (Sissa Medialab, 2018).
  - [9] J. Maldacena and A. Milekhin, SYK wormhole formation in real time, *JHEP* **04**, 258, [arXiv:1912.03276](https://arxiv.org/abs/1912.03276) [hep-th].
  - [10] D. A. Trunin, Pedagogical introduction to the Sachdev-Ye-Kitaev model and two-dimensional dilaton gravity, *Physics-Uspekhi* **64**, 219–252 (2021).
  - [11] D. Chowdhury, A. Georges, O. Parcollet, and S. Sachdev, Sachdev-Ye-Kitaev models and beyond: Window into non-Fermi liquids, *Rev. Mod. Phys.* **94**, 035004 (2022).
  - [12] R. Bousso, X. Dong, N. Engelhardt, T. Faulkner, T. Hartman, S. H. Shenker, and D. Stanford, *Snowmass White Paper: Quantum Aspects of Black Holes and the Emergence of Spacetime* (2022), [arXiv:2201.03096](https://arxiv.org/abs/2201.03096) [hep-th].
  - [13] T. Faulkner, T. Hartman, M. Headrick, M. Rangamani, and B. Swingle, *Snowmass white paper: Quantum information in quantum field theory and quantum gravity* (2022), [arXiv:2203.07117](https://arxiv.org/abs/2203.07117) [hep-th].
  - [14] S. Catterall, R. Harnik, V. E. Hubeny, C. W. Bauer, A. Berlin, Z. Davoudi, T. Faulkner, T. Hartman, M. Headrick, Y. F. Kahn, H. Lamm, Y. Meurice, S. Rajendran, M. Rangamani, and B. Swingle, *Report of the Snowmass 2021 Theory Frontier Topical Group on Quantum Information Science* (2022), [arXiv:2209.14839](https://arxiv.org/abs/2209.14839) [quant-ph].
  - [15] T. Schuster, B. Kobrin, P. Gao, I. Cong, E. T. Khabiboulline, N. M. Linke, M. D. Lukin, C. Monroe, B. Yoshida, and N. Y. Yao, Many-Body Quantum Teleportation via Operator Spreading in the Traversable Wormhole Protocol, *Physical Review X* **12** (2022).
  - [16] L. E. Anderson, A. Laitinen, A. Zimmerman, T. Werkmeister, H. Shackleton, A. Kruchkov, T. Taniguchi, K. Watanabe, S. Sachdev, and P. Kim, Magneto-Thermoelectric Transport in Graphene Quantum Dot with Strong Correlations, *Phys. Rev. Lett.* **132** (2024).
  - [17] I. Danshita, M. Hanada, and M. Tezuka, Creating and probing the Sachdev-Ye-Kitaev model with ultracold gases: Towards experimental studies of quantum gravity, *Progress of Theoretical and Experimental Physics* **2017**, 083I01 (2017), [arXiv:1606.02454](https://arxiv.org/abs/1606.02454) [quant-ph].
  - [18] L. García-Álvarez, I. L. Egusquiza, L. Lamata, A. del Campo, J. Sonner, and E. Solano, Digital Quantum Simulation of Minimal AdS/CFT, *Phys. Rev. Lett.* **119**, 040501 (2017), [arXiv:1607.08560](https://arxiv.org/abs/1607.08560) [quant-ph].
  - [19] M. Franz and M. Rozali, Mimicking black hole event horizons in atomic and solid-state systems, *Nature Rev. Mater.* **3**, 491 (2018), [arXiv:1808.00541](https://arxiv.org/abs/1808.00541) [cond-mat.str-el].
  - [20] Z. Luo, Y.-Z. You, J. Li, C.-M. Jian, D. Lu, C. Xu, B. Zeng, and R. Laflamme, Quantum simulation of the non-fermi-liquid state of Sachdev-Ye-Kitaev model, *npj Quantum Information* **5** (2019).
  - [21] D. Jafferis, A. Zlokapa, J. D. Lykken, D. K. Kolchmeyer, S. I. Davis, N. Lauk, H. Neven, and M. Spiropulu, Traversable wormhole dynamics on a quantum processor, *Nature* **612**, 51 (2022).
  - [22] B. Kobrin, T. Schuster, and N. Y. Yao, *Comment on "traversable wormhole dynamics on a quantum processor"* (2023), [arXiv:2302.07897](https://arxiv.org/abs/2302.07897) [quant-ph].
  - [23] M. Asaduzzaman, R. G. Jha, and B. Sambasivam, Sachdev-Ye-Kitaev model on a noisy quantum computer, *Phys. Rev. D* **109**, 105002 (2024), [arXiv:2311.17991](https://arxiv.org/abs/2311.17991) [quant-ph].
  - [24] S. Xu, L. Susskind, Y. Su, and B. Swingle, A Sparse Model of Quantum Holography, [arXiv:2008.02303](https://arxiv.org/abs/2008.02303) [cond-mat.str-el].
  - [25] E. Cáceres, A. Misobuchi, and R. Pimentel, Sparse SYK and traversable wormholes, *JHEP* **11**, 015.
  - [26] A. M. García-García, Y. Jia, D. Rosa, and J. J. M. Verbaarschot, Sparse Sachdev-Ye-Kitaev model, quantum chaos, and gravity duals, *Phys. Rev. D* **103**, 106002 (2021).
  - [27] T. Anegawa, N. Iizuka, A. Mukherjee, S. K. Sake, and S. P. Trivedi, Sparse random matrices and Gaussian ensembles with varying randomness, *Journal of High Energy Physics* **2023** (2023).
  - [28] E. Cáceres, T. Guglielmo, B. Kent, and A. Misobuchi, Out-of-time-order correlators and Lyapunov exponents in sparse SYK, *JHEP* **11**, 088.
  - [29] P. Orman, H. Gharibyan, and J. Preskill, *Quantum chaos in the sparse SYK model* (2024), [arXiv:2403.13884](https://arxiv.org/abs/2403.13884) [hep-th].
  - [30] M. Tezuka, O. Oktay, E. Rinaldi, M. Hanada, and F. Nori, Binary-coupling sparse Sachdev-Ye-Kitaev model: An improved model of quantum chaos and holography, *Phys. Rev. B* **107**, L081103 (2023).
  - [31] B. Swingle and M. Winer, Bosonic model of quantum holography, *Phys. Rev. B* **109**, 094206 (2024),

- arXiv:2311.01516 [hep-th].
- [32] M. Hanada, A. Jevicki, X. Liu, E. Rinaldi, and M. Tezuka, A model of randomly-coupled Pauli spins, *Journal of High Energy Physics* **2024** (2024), arXiv:2309.15349 [hep-th].
  - [33] J. B. French and S. S. M. Wong, Validity of random matrix theories for many-particle systems, *Phys. Lett. B* **33**, 449 (1970).
  - [34] O. Bohigas and J. Flores, Two-body random Hamiltonian and level density, *Phys. Lett. B* **34**, 261 (1971).
  - [35] S. Sachdev, Bekenstein-Hawking Entropy and Strange Metals, *Phys. Rev. X* **5**, 041025 (2015).
  - [36] J. C. Louw and S. Kehrein, Thermalization of many many-body interacting Sachdev-Ye-Kitaev models, *Phys. Rev. B* **105**, 075117 (2022).
  - [37] C. Zanoci and B. Swingle, Near-equilibrium approach to transport in complex Sachdev-Ye-Kitaev models, *Phys. Rev. B* **105**, 235131 (2022).
  - [38] R. A. Davison, W. Fu, A. Georges, Y. Gu, K. Jensen, and S. Sachdev, Thermoelectric transport in disordered metals without quasiparticles: The Sachdev-Ye-Kitaev models and holography, *Phys. Rev. B* **95**, 155131 (2017).
  - [39] Y. Gu, A. Kitaev, S. Sachdev, and G. Tarnopolsky, Notes on the complex Sachdev-Ye-Kitaev model, *Journal of High Energy Physics* **2020** (2020).
  - [40] H. Wang, A. L. Chudnovskiy, A. Gorsky, and A. Kamenev, Sachdev-Ye-Kitaev superconductivity: Quantum Kuramoto and generalized Richardson models, *Phys. Rev. Res.* **2**, 033025 (2020).
  - [41] W. Fu and S. Sachdev, Numerical study of fermion and boson models with infinite-range random interactions, *Phys. Rev. B* **94**, 035135 (2016).
  - [42] T. Scaffidi and E. Altman, Chaos in a classical limit of the Sachdev-Ye-Kitaev model, *Phys. Rev. B* **100**, 155128 (2019).
  - [43] D. J. Gross and V. Rosenhaus, A generalization of Sachdev-Ye-Kitaev, *Journal of High Energy Physics* **2017** (2017).
  - [44] W. Fu, D. Gaiotto, J. Maldacena, and S. Sachdev, Supersymmetric Sachdev-Ye-Kitaev models, *Phys. Rev. D* **95**, 026009 (2017).
  - [45] T. Li, J. Liu, Y. Xin, and Y. Zhou, Supersymmetric SYK model and random matrix theory, *Journal of High Energy Physics* **2017** (2017).
  - [46] F. Sun and J. Ye, Periodic table of the ordinary and supersymmetric Sachdev-Ye-Kitaev models, *Phys. Rev. Lett.* **124**, 244101 (2020).
  - [47] S. J. Gates, Y. Hu, and S.-N. H. Mak, On 1-D,  $\mathcal{N} = 4$  supersymmetric SYK-type models. part I, *Journal of High Energy Physics* **2021** (2021).
  - [48] A. M. García-García, L. Sá, and J. J. M. Verbaarschot, Symmetry classification and universality in non-hermitian many-body quantum chaos by the Sachdev-Ye-Kitaev model, *Phys. Rev. X* **12**, 021040 (2022).
  - [49] G. Cipolloni and J. Kudler-Flam, Entanglement Entropy of Non-Hermitian Eigenstates and the Ginibre Ensemble, *Phys. Rev. Lett.* **130**, 010401 (2023).
  - [50] P. Nandy, T. Pathak, and M. Tezuka, Probing quantum chaos through singular-value correlations in the sparse non-Hermitian Sachdev-Ye-Kitaev model, *Phys. Rev. B* **111**, L060201 (2025), arXiv:2406.11969 [quant-ph].
  - [51] J. Maldacena and X.-L. Qi, Eternal traversable worm-hole (2018), arXiv:1804.00491 [hep-th].
  - [52] Y. Jia, D. Rosa, and J. J. M. Verbaarschot, Replica symmetry breaking for the integrable two-site Sachdev-Ye-Kitaev model, *Journal of Mathematical Physics* **63** (2022).
  - [53] M. Berkooz, P. Narayan, M. Rozali, and J. Simón, Higher dimensional generalizations of the SYK model, *Journal of High Energy Physics* **2017** (2017).
  - [54] Y. Gu, X.-L. Qi, and D. Stanford, Local criticality, diffusion and chaos in generalized Sachdev-Ye-Kitaev models, *Journal of High Energy Physics* **2017** (2017).
  - [55] M. Berkooz, M. Isachenkov, V. Narovlansky, and G. Torrents, Towards a full solution of the large  $N$  double-scaled SYK model, *JHEP* **03**, 079, arXiv:1811.02584 [hep-th].
  - [56] M. Berkooz, P. Narayan, and J. Simon, Chord diagrams, exact correlators in spin glasses and black hole bulk reconstruction, *JHEP* **08**, 192, arXiv:1806.04380 [hep-th].
  - [57] S. Ozaki and H. Katsura, Disorder-free sachdev-ye-kitaev models: Integrability and a precursor of chaos, *Phys. Rev. Res.* **7**, 013092 (2025).
  - [58] W. Wang, A. Davis, G. Pan, Y. Wang, and Z. Y. Meng, Phase diagram of the spin- $\frac{1}{2}$  Yukawa-Sachdev-Ye-Kitaev model: Non-Fermi liquid, insulator, and superconductor, *Phys. Rev. B* **103**, 195108 (2021).
  - [59] S. Sachdev, Holographic Metals and the Fractionalized Fermi Liquid, *Phys. Rev. Lett.* **105**, 151602 (2010).
  - [60] X.-Y. Song, C.-M. Jian, and L. Balents, Strongly correlated metal built from Sachdev-Ye-Kitaev models, *Phys. Rev. Lett.* **119**, 216601 (2017).
  - [61] F. Monteiro, M. Tezuka, A. Altland, D. A. Huse, and T. Micklitz, Quantum ergodicity in the many-body localization problem, *Physical Review Letters* **127**, 10.1103/physrevlett.127.030601 (2021).
  - [62] Y. Nakata and M. Tezuka, Hayden-Preskill recovery in Hamiltonian systems, *Physical Review Research* **6** (2024), arXiv:2303.02010 [cond-mat.str-el].
  - [63] L. Amico, R. Fazio, A. Osterloh, and V. Vedral, Entanglement in many-body systems, *Rev. Mod. Phys.* **80**, 517 (2008).
  - [64] X. Wang, S. Ghose, B. C. Sanders, and B. Hu, Entanglement as a signature of quantum chaos, *Physical Review E* **70** (2004).
  - [65] L. F. Santos, G. Rigolin, and C. O. Escobar, Entanglement versus chaos in disordered spin chains, *Physical Review A* **69** (2004).
  - [66] J. N. Bandyopadhyay and A. Lakshminarayanan, Entanglement production in coupled chaotic systems: Case of the kicked tops, *Phys. Rev. E* **69** (2004).
  - [67] J. Karthik, A. Sharma, and A. Lakshminarayanan, Entanglement, avoided crossings, and quantum chaos in an Ising model with a tilted magnetic field, *Physical Review A* **75** (2007).
  - [68] S. Dogra, V. Madhok, and A. Lakshminarayanan, Quantum signatures of chaos, thermalization, and tunneling in the exactly solvable few-body kicked top, *Phys. Rev. E* **99** (2019).
  - [69] C. M. Trail, V. Madhok, and I. H. Deutsch, Entanglement and the generation of random states in the quantum chaotic dynamics of kicked coupled tops, *Physical Review E* **78** (2008).
  - [70] L. Vidmar and M. Rigol, Entanglement Entropy of Eigenstates of Quantum Chaotic Hamiltonians, *Phys. Rev. Lett.* **119**, 220603 (2017).
  - [71] P. Łydzba, M. Rigol, and L. Vidmar, Eigenstate en-

- tanglement entropy in random quadratic Hamiltonians, *Phys. Rev. Lett.* **125**, 180604 (2020).
- [72] W. H. Zurek and J. P. Paz, Quantum chaos: A decoherent definition, *Physica D* **83**, 300 (1995), [arXiv:quant-ph/9502029](#).
- [73] K. Furuya, M. C. Nemes, and G. Q. Pellegrino, Quantum dynamical manifestation of chaotic behavior in the process of entanglement, *Phys. Rev. Lett.* **80**, 5524 (1998).
- [74] P. A. Miller and S. Sarkar, Signatures of chaos in the entanglement of two coupled quantum kicked tops, *Phys. Rev. E* **60**, 1542 (1999).
- [75] A. Lakshminarayan, Entangling power of quantized chaotic systems, *Phys. Rev. E* **64**, 036207 (2001).
- [76] P. Zanardi, C. Zalka, and L. Faoro, Entangling power of quantum evolutions, *Phys. Rev. A* **62**, 030301 (2000), [arXiv:quant-ph/0005031](#).
- [77] P. Zanardi, Entanglement of quantum evolutions, *Physical Review A* **63**, 10.1103/physreva.63.040304 (2001), [arXiv:quant-ph/0010074 \[quant-ph\]](#).
- [78] A. J. Scott and C. M. Caves, Entangling power of the quantum baker's map, *Journal of Physics A: Mathematical and General* **36**, 9553–9576 (2003).
- [79] A. J. Scott, Multipartite entanglement, quantum-error-correcting codes, and entangling power of quantum evolutions, *Physical Review A* **69** (2004).
- [80] J. N. Bandyopadhyay and A. Lakshminarayan, Entangling power of quantum chaotic evolutions via operator entanglement (2005), [arXiv:quant-ph/0504052 \[quant-ph\]](#).
- [81] R. F. Abreu and R. O. Vallejos, Entangling power of the baker's map: Role of symmetries, *Physical Review A* **73**, 10.1103/physreva.73.052327 (2006).
- [82] J. N. Bandyopadhyay and A. Lakshminarayan, Testing Statistical Bounds on Entanglement Using Quantum Chaos, *Phys. Rev. Lett.* **89** (2002).
- [83] A. Lahiri and S. Nag, Dynamical manifestation of quantum chaos: density matrix fluctuations in subsystems, *Physics Letters A* **318**, 6 (2003).
- [84] A. Lahiri, Dynamical criterion for quantum chaos: Entropy production in subsystems, [arXiv preprint quant-ph/0302029](#) (2003).
- [85] H. Gharibyan, M. Hanada, B. Swingle, and M. Tezuka, Quantum Lyapunov spectrum, *Journal of High Energy Physics* **2019**, 10.1007/jhep04(2019)082 (2019).
- [86] M. L. Mehta, *Random matrices* (Elsevier, 2004).
- [87] S. Tomsovic, A. Lakshminarayan, S. C. L. Srivastava, and A. Bäcker, Eigenstate entanglement between quantum chaotic subsystems: Universal transitions and power laws in the entanglement spectrum, *Physical Review E* **98** (2018).
- [88] See Supplemental Material at URL-will-be-inserted-by-publisher, with additional references [91, 99–107], for details on numerics and additional supporting results.
- [89] D. N. Page, Average entropy of a subsystem, *Phys. Rev. Lett.* **71**, 1291 (1993), [arXiv:gr-qc/9305007](#).
- [90] S. Sen, Average Entropy of a Quantum Subsystem, *Physical Review Letters* **77**, 1–3 (1996).
- [91] H. Kim and D. A. Huse, Ballistic Spreading of Entanglement in a Diffusive Nonintegrable System, *Phys. Rev. Lett.* **111**, 127205 (2013).
- [92] We would like to emphasize that the results in our study are for the fixed initial product(maximally entangled) state chosen. In general it is possible to study by choosing ensemble of appropriate product states [76, 108] and averaging over their ensemble.
- [93] M. Tezuka, O. Oktay, E. Rinaldi, M. Hanada, and F. Nori, Binary-coupling sparse Sachdev–Ye–Kitaev model: An improved model of quantum chaos and holography, *Phys. Rev. B* **107**, L081103 (2023).
- [94] T. Hartman and J. Maldacena, Time Evolution of Entanglement Entropy from Black Hole Interiors, *JHEP* **05**, 014, [arXiv:1303.1080 \[hep-th\]](#).
- [95] H. Liu and S. J. Suh, Entanglement Tsunami: Universal Scaling in Holographic Thermalization, *Phys. Rev. Lett.* **112**, 011601 (2014), [arXiv:1305.7244 \[hep-th\]](#).
- [96] H. Liu and S. J. Suh, Entanglement growth during thermalization in holographic systems, *Phys. Rev. D* **89**, 066012 (2014), [arXiv:1311.1200 \[hep-th\]](#).
- [97] P. Hosur, X.-L. Qi, D. A. Roberts, and B. Yoshida, Chaos in quantum channels, *JHEP* **02**, 004, [arXiv:1511.04021 \[hep-th\]](#).
- [98] M. Hanada, S. van Leuven, O. Oktay, and M. Tezuka, Two-local modifications of SYK model with quantum chaos (2025), [arXiv:2505.09900 \[quant-ph\]](#).
- [99] M. C. Bañuls, J. I. Cirac, and M. B. Hastings, Strong and Weak Thermalization of Infinite Nonintegrable Quantum Systems, *Phys. Rev. Lett.* **106**, 050405 (2011).
- [100] L. Zhang, H. Kim, and D. A. Huse, Thermalization of entanglement, *Phys. Rev. E* **91**, 062128 (2015).
- [101] D. A. Roberts, D. Stanford, and L. Susskind, Localized shocks, *JHEP* **03**, 051, [arXiv:1409.8180 \[hep-th\]](#).
- [102] B. Craps, M. De Clerck, D. Janssens, V. Luyten, and C. Rabideau, Lyapunov growth in quantum spin chains, *Phys. Rev. B* **101**, 174313 (2020).
- [103] J. F. Rodriguez-Nieva, C. Jonay, and V. Khemani, Quantifying Quantum Chaos through Microcanonical Distributions of Entanglement, *Phys. Rev. X* **14**, 031014 (2024), [arXiv:2305.11940 \[cond-mat.stat-mech\]](#).
- [104] I. Kukuljan, S. Grozdanov, and T. Prosen, Weak quantum chaos, *Physical Review B* **96**, 060301 (2017).
- [105] V. Khemani, D. A. Huse, and A. Nahum, Velocity-dependent Lyapunov exponents in many-body quantum, semiclassical, and classical chaos, *Phys. Rev. B* **98**, 144304 (2018).
- [106] S. Xu and B. Swingle, Locality, Quantum Fluctuations, and Scrambling, *Phys. Rev. X* **9**, 031048 (2019).
- [107] B. V. Fine, T. A. Elsayed, C. M. Kropf, and A. S. de Wijn, Absence of exponential sensitivity to small perturbations in nonintegrable systems of spins 1/2, *Phys. Rev. E* **89**, 012923 (2014).
- [108] R. Demkowicz-Dobrzański and M. Kuś, Global entangling properties of the coupled kicked tops, *Phys. Rev. E* **70**, 066216 (2004).

# Supplemental Materials: Entanglement production in the Sachdev–Ye–Kitaev Model and its variants

Tanay Pathak and Masaki Tezuka

## A. Fixing the variance of eigenvalues

We now provide the method to fix the variance across all the models and random matrices considered. It is important to fix the energy scales, which we achieve by fixing the variance, to ensure proper comparison of the models. We first note a few properties of the random matrices belonging to Gaussian orthogonal ensemble (GOE) and Gaussian Unitary ensemble (GUE).

GOE type random matrices are real Hermitian matrices with entries chosen, upto symmetry, from Gaussian distribution with variance 1 along the diagonal and variance 1/2 along the off-diagonals. Similarly, GUE type random matrices are Hermitian matrices with complex entries (upto Hermiticity) with both real and imaginary parts chosen from Gaussian distribution with variance 1/2.

Now, using the property that for a given  $\mathcal{D} \times \mathcal{D}$  dimensional matrix  $H$  its trace can be written as  $\text{Tr}(H^2) = \sum_{m=1}^{\mathcal{D}} \sum_{n=1}^{\mathcal{D}} H_{mn}^2$  we can calculate the expectation value of  $\mathbb{E}(\text{Tr}(H^2))$  for both ensembles. We then have

$$\mathbb{E}(\text{Tr}(H_{\text{GOE}}^2)) = \sum_i \mathbb{E}((\lambda_{\text{goe}})_i^2) = \frac{\mathcal{D}(\mathcal{D} + 1)}{2} \quad (\text{A1})$$

$$\mathbb{E}(\text{Tr}(H_{\text{GUE}}^2)) = \sum_i \mathbb{E}((\lambda_{\text{gue}})_i^2) = \mathcal{D}^2. \quad (\text{A2})$$

where  $\lambda_i$  denotes the eigenvalue of the corresponding random matrix. For the SYK model (all the variants), with  $N$  fermion and  $q = 4$ , using the property of Majorana operator we can calculate the expectation value of trace of hamiltonian squared as

$$\mathbb{E}(\text{Tr}(H_{\text{GOE}}^2)) = \sum_i \mathbb{E}((\lambda_{\text{SYK}})_i^2) = \frac{6 \cdot 2^{N/2} \binom{N}{4}}{2^4 N^3} \quad (\text{A3})$$

Using these properties we can calculate the variance of eigenvalues, and we get the following:

$$\sigma_{\text{GOE}}^2 = \frac{(\mathcal{D} + 1)}{2} \quad \sigma_{\text{GUE}}^2 = \mathcal{D}, \quad \sigma_{\text{SYK}}^2 = \frac{6 \cdot 2^{N/2} \binom{N}{4}}{2^{4+N/2} N^3} \quad (\text{A4})$$

Using these properties we can easily fix the variance of the corresponding semicircle eigenvalue density. As an example of the above implementation consider we want to match the variance of GOE random matrix with SYK model having  $n$  Majorana fermions<sup>1</sup>. In MATHEMATICA one can use the command `RandomVariate[GaussianUnitaryMatrixDistribution[1, 2n/2]` to generate a random matrix of GOE type. We then multiply the generated matrix with the prefactor  $\frac{1}{2^{n/2}} \sqrt{\frac{6 \cdot 2^n \binom{2n}{4}}{2^4 (2n)^3 2^n}}$ . This will fix the variance automatically. Other cases can be dealt with in a similar manner. Notice that this procedure is strictly valid for large-dimensional random matrices and one will see differences at small sizes due to the comparable finite size corrections to the semicircle eigenvalue density.

## B. Results for random matrices

In this appendix, we provide the numerical results for the average entanglement entropy (EE) of the eigenstates of Gaussian random matrices belong to orthogonal (GOE), unitary (GUE) and symplectic (GSE) class. The bound for

---

<sup>1</sup> We avoid using `N` as it is an internal command in MATHEMATICA.

average entanglement entropy for such eigenstates using RMT is given as

$$\langle S_E \rangle \cong \ln(\mathcal{N}) - \frac{\mathcal{N}}{2M} \quad (\text{B1})$$

These results are shown in Fig. 5. The mean of the average EE over the whole spectrum (and 50 Hamiltonian realization) we obtain are:  $\langle S \rangle_{\text{GSE}} = 3.659$ ,  $\langle S \rangle_{\text{GUE}} = 3.659$ ,  $\langle S \rangle_{\text{GOE}} = 3.653$  for GSE, GUE and GOE respectively while using the Eq.(B1) we obtain  $\langle S \rangle = 3.65888$ . We see a slightly better agreement with the GSE and GUE cases. For the GUE case it can be attributed to the sensitivity of entanglement spectrum to the breaking of time-reversal symmetry as was briefly mentioned in [75] as well. The EE is sensitive to symmetries of the underlying model and time reversal breaking interaction may produce more entanglement on average and reduced density matrix are sensitive to it.

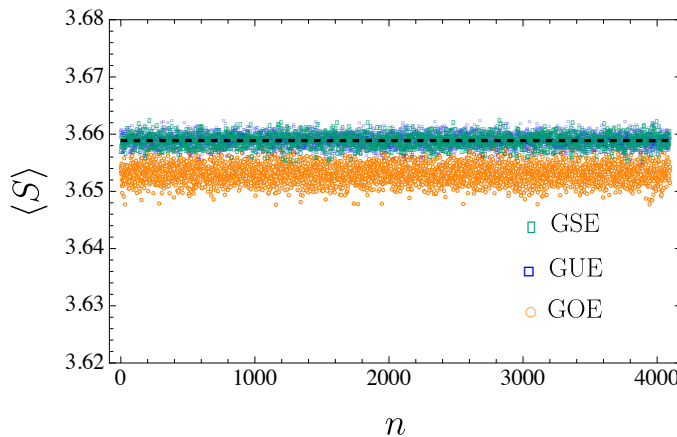


FIG. 5.  $\langle S \rangle$  of the eigenstates, indexed using  $n$ , of GSE, GUE and GOE type random matrices, for  $l = 1/2$  sub-system fraction. The horizontal black line corresponds to the analytical bound on entropy and the horizontal three different markers corresponds to the numerically obtained result for GSE, GUE and GOE respectively. We take matrices of dimensions  $2^{12}$  and averaging is done over 50 realizations (for each index  $n$ ). Observe that the results for GSE and GUE are on average much closer as compared to GOE, to the theoretical value given by Eq. (B1).

The following states are used as the product and the maximally entangled initial states:

$$\Psi_P = \bigotimes_{i=1}^n \frac{1}{\sqrt{2}}(|0\rangle + |1\rangle), \quad (\text{B2})$$

$$\Psi_M = \frac{1}{\sqrt{n}} \sum_{i=1}^n (|i\rangle \otimes |i\rangle), \quad (\text{B3})$$

where in  $\Psi_M$ ,  $|1\rangle = (1, 0, 0, \dots, 0)$ ,  $|2\rangle = (0, 1, 0, \dots, 0)$  and so on denotes a  $n$ -level basis state.

In Fig. 6(left) (a) we provide the results of the evolution of initial product state  $\Psi_P$ . Fig. 6(left) (b)-(e) show the result for the maximally entangled initial state  $\Psi_M$  which is evolved using a GOE type random matrix of dimension  $\mathcal{D} = 2^{12}$ , for various values of subsystem fraction  $l$ . The averaging is done over 50 Hamiltonian realizations. We observe a good agreement between the saturation value and the theoretical limit. As was briefly discussed in the main text, we also observe that the bound is saturated for both  $\Psi_P$  and  $\Psi_M$ . For the case of  $\Psi_M$ , as the initial state is already maximally entangled, the entanglement entropy first decreases (the state gets slightly disentangled) and then saturates to the theoretical value given by Eq. (B1). In Fig. 6 (f)-(j), the results are shown for the GUE with similar conclusions.

### C. Derivation of the entanglement bound

The final result obtained in this section is already stated in [87] and can also be easily obtained from the result derived in [89, 90]. We however re-derive the result here again for the convenience of the readers.

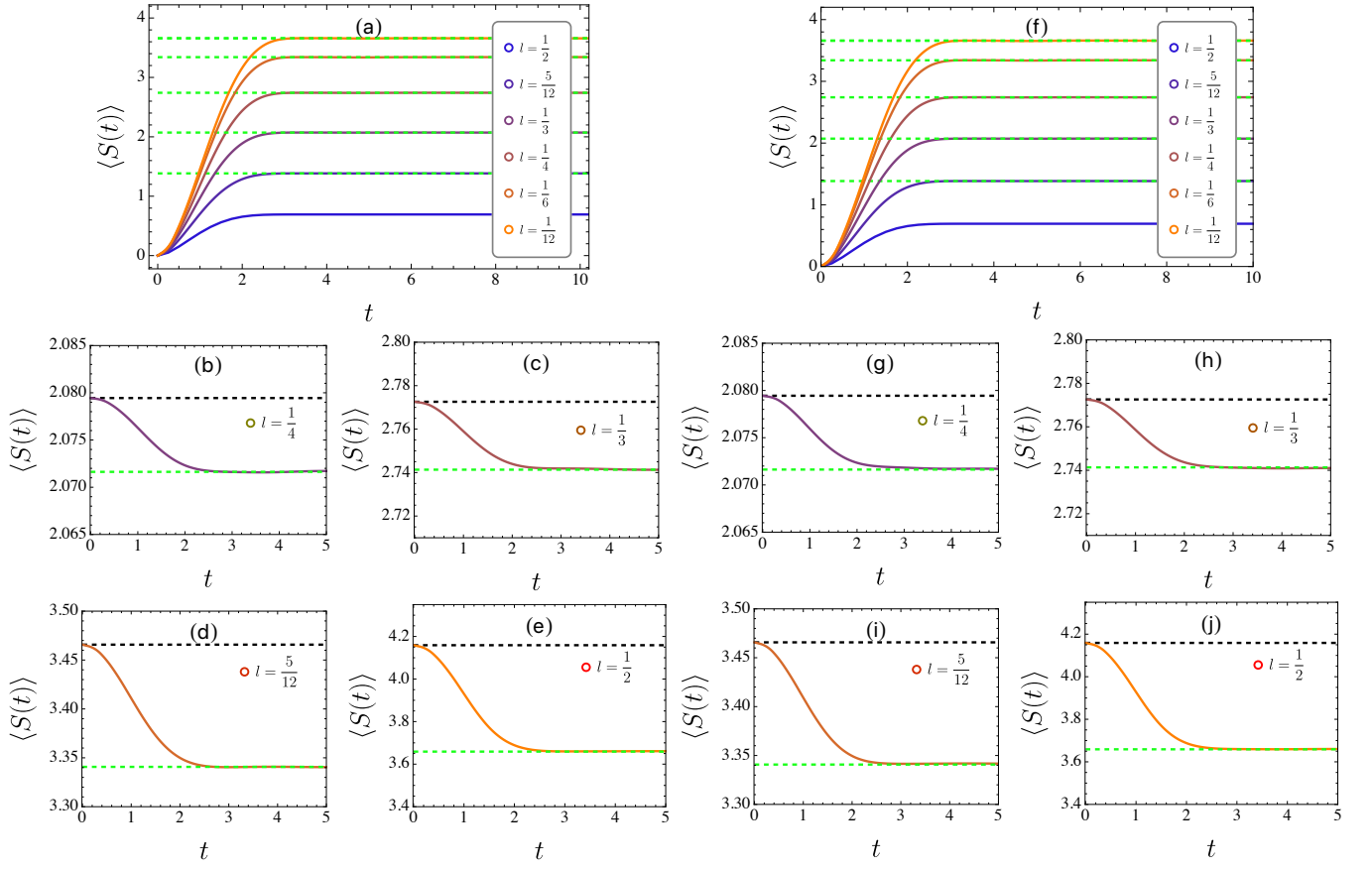


FIG. 6. (Left) (a) Evolution of EE for an initial product state with time, for various sub-system fractions, for the GOE case. (b), (c), (d), (e) show the EE evolution, using GOE matrices, of maximally entangled state with subsystem fraction  $l = 1/4, 1/3, 5/12, 1/2$ . The horizontal dashed black line corresponds to the maximal value of entropy and the horizontal green line corresponds to the analytical result given by either Eq. (B1). (Right) (f) Evolution of EE for an initial product state with time, for various sub-system fractions, for the GUE case. (g), (h), (i), (j) show the EE evolution, using GUE matrices, of maximally entangled state with subsystem fraction  $l = 1/4, 1/3, 5/12, 1/2$ . The horizontal dashed black line corresponds to the maximal value of entropy and the horizontal green line corresponds to the analytical result given by either Eq. (B1). We take  $\mathcal{D} = 2^{12}$  and averaging is done over 50 realizations.

Consider a bi-partition of Hilbert space  $\mathcal{H} = \mathcal{H}_A \otimes \mathcal{H}_B$ , of dimension  $\mathcal{D}$ . We have in general  $\dim(\mathcal{H}_A) = \mathcal{M}$  and  $\dim(\mathcal{H}_B) = \mathcal{N}$ ,  $\mathcal{D} = \mathcal{M} \otimes \mathcal{N}$ . Consider the density matrix  $\rho \in \mathcal{H}$ . The reduced density matrix (RDM) obtained after tracing over subsystem  $A$  is given by  $\rho_B = \text{Tr}_A(\rho)$  and similarly we have  $\rho_A = \text{Tr}_B(\rho)$  obtained from the full density matrix after tracing over subsystem  $B$ . The ensemble of the reduced density matrix is the trace restricted Wishart ensemble (trace being unity).

The average density of states of ensemble of Wishart matrices is given by the Marchenko–Pastur distribution [86]

$$f(\epsilon) = \frac{\mathcal{N}Q}{2\pi} \frac{\sqrt{(\epsilon_{\max} - \epsilon)(\epsilon - \epsilon_{\min})}}{\epsilon},$$

$$\epsilon_{\min}^{\max} = \frac{1}{\mathcal{N}} \left( 1 + \frac{1}{Q} \pm \frac{2}{\sqrt{Q}} \right) \quad (\text{C1})$$

where  $\epsilon \in [\epsilon_{\min}, \epsilon_{\max}]$  and  $Q = \mathcal{M}/\mathcal{N}$ .

Using this, in [82] a bound on the average entanglement entropy was proposed, which is

$$\langle S_E \rangle \cong - \int_{\epsilon_{\min}}^{\epsilon_{\max}} f(\epsilon) \epsilon \ln(\epsilon) d\epsilon \equiv \ln(\gamma \mathcal{N}). \quad (\text{C2})$$

The von Neumann entropy is then given by

$$S(\rho_A) = -\text{Tr}(\rho_A \ln(\rho_A)) = -\sum_{i=1}^{\mathcal{N}} \epsilon_i \ln(\epsilon_i) \quad (\text{C3})$$

and similarly for  $\rho_B$ . We will now give an alternative derivation of the integral given by Eq. (C2).

We instead consider the following integral which is closely related to Eq. (C2)

$$I = \int_a^b \sqrt{(x-a)(b-a)} \ln(x) dx. \quad (\text{C4})$$

The integral is not straightforward to evaluate in the present form due to the presence of the logarithm function. We try to simplify the integral using the following

$$\begin{aligned} \frac{d}{dx}(x^\epsilon) &= x^\epsilon \ln(x) \\ \Rightarrow \frac{d}{dx}(x^\epsilon) \Big|_{\epsilon \rightarrow 0} &= \ln(x) \end{aligned} \quad (\text{C5})$$

We thus re-write the integral in Eq. (C4)

$$I = \frac{d}{dx} \left( \int_a^b \sqrt{(x-a)(b-x)} x^\epsilon dx \right) \Big|_{\epsilon \rightarrow 0} \quad (\text{C6})$$

We now have a simpler integral to evaluate. The above integral can be evaluated in terms of hypergeometric function (using MATHEMATICA) and we obtain

$$\int_a^b \sqrt{(x-a)(b-x)} x^\epsilon dx = \frac{a^{\epsilon-1} \left( \pi a(a+b) {}_2F_1\left(-\frac{1}{2}, 1-\epsilon; 1; 1-\frac{b}{a}\right) - \pi b(2a\epsilon + a - 2b\epsilon + b) {}_2F_1\left(\frac{1}{2}, 1-\epsilon; 1; 1-\frac{b}{a}\right) \right)}{4\epsilon(\epsilon+1)} \quad (\text{C7})$$

The next step to evaluate  $I$  is to take the derivative of the above result and take the limit  $\epsilon \rightarrow 0$ . Using the integral representation of the  ${}_2F_1$  hypergeometric integral we get the following

$$\frac{d}{dx} \left( {}_2F_1\left(\frac{1}{2}, 1-\epsilon; 1; 1-\frac{b}{a}\right) \right) \Big|_{\epsilon=0} = 2 \log \left( \frac{2}{\sqrt{\frac{b}{a}} + 1} \right), \quad (\text{C8})$$

$$\frac{d}{dx} \left( {}_2F_1\left(-\frac{1}{2}, 1-\epsilon; 1; 1-\frac{b}{a}\right) \right) \Big|_{\epsilon=0} = 2 \left( -1 + \log \left( \frac{2}{\sqrt{\frac{b}{a}} + 1} \right) + \sqrt{\frac{b}{a}} \right). \quad (\text{C9})$$

Using these results we obtain the result of integral in Eq. (C4) as follows

$$I = \frac{1}{16} \pi \left( -4a^2 \sqrt{\frac{b}{a}} + a^2 + 6ab - 4ab \sqrt{\frac{b}{a}} - 4 \log(2)(a-b)^2 + 2(a-b)^2 \log \left( \left( \sqrt{a} + \sqrt{b} \right)^2 \right) + b^2 \right) \quad (\text{C10})$$

It is now straightforward to evaluate the integral in Eq. (C2). We get a remarkably simpler result for  $I$  as compared to the result previously stated (in [82]).

$$S = \ln(\mathcal{N}) - \frac{1}{2Q} = \ln(\mathcal{N}) - \frac{\mathcal{N}}{2\mathcal{M}}. \quad (\text{C11})$$

We remark that the above result is not new but it is the Page's result [89] for the entanglement entropy of a random pure state in the limit  $Q \gg 1$ .

## D. More results for SYK model

In this section we present results for different types of SYK model for various other value of sparseness, which are not shown in the main text.

### 1. The SYK model

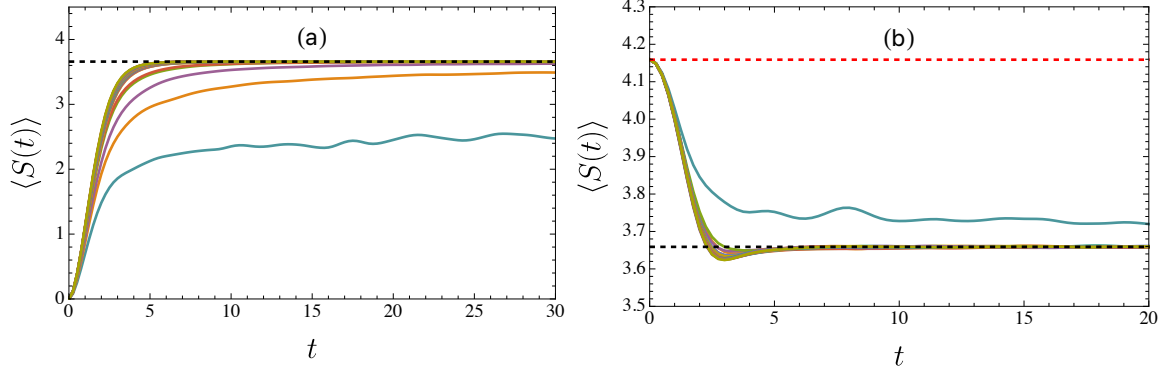


FIG. 7. (a) EE evolution of a product state with time, for various system fractions. The horizontal black line corresponds to the analytical result given by either Eq. (C2) or Eq. (1). We take  $N = 24$  and averaging is done over 50 realizations. We take values as  $p = 0.001, 0.002, 0.003, 0.004, 0.005, 0.01, 0.012, 0.013, 0.014, 0.015, 0.016, 0.017, 0.018, 0.019, 0.02, 0.03, 0.04, 0.05, 0.06, 0.07, 0.08, 0.1, 0.25, 0.5, 1$ . (b) EE evolution of a maximally entangled state with time, for various system fractions. The horizontal black line corresponds to the analytical result given by either Eq. (1). We take  $N = 24$  and averaging is done over 50 realizations. The critical value of  $p$  after which the the entanglement entropy does not reach the theoretical bound, for initial product state, is  $p_c = 0.004$ . For the case when initial state is a maximally entangled state  $p_c = 0.001$

### 2. The Binary SYK model

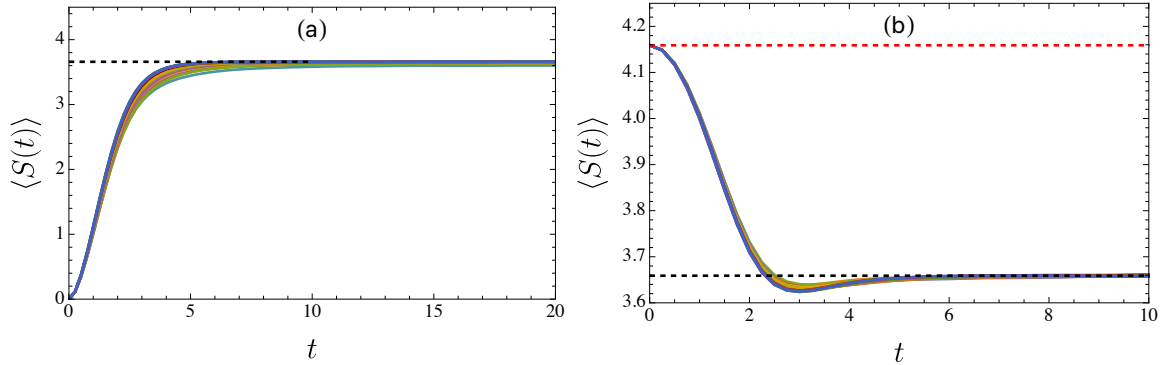


FIG. 8. (a) EE evolution of a product state with time, for various system fractions, for binary sparse SYK model. The horizontal black line corresponds to the analytical result given by either Eq. (C2) or Eq. (1). We take  $N = 24$  and averaging is done over 50 realizations. We take values as  $\kappa = 18, 20, 22, 24, 26, 28, 30, 32, 34, 36, 38, 40, 100, 600, 900, 1500, 3500, 6500, 10626$ . (b) EE evolution of a maximally entangled state with time, for various system fractions. The horizontal black line corresponds to the analytical result given by either Eq. (1). We take  $N = 24$  and averaging is done over 50 realizations. Observe how even for  $\kappa = 18$  ( $p \approx 0.001$ ) the curves are still very close to the  $\kappa = 10626$  curve, for both kinds of initial states. The critical value of  $\kappa$  after which the the entanglement entropy does not reach the theoretical bound is  $k_c = 22$  or  $p_c = 0.002$ . For the case when initial state is a maximally entangled state we find that even for the smallest  $\kappa$  ( $=18$ ) the bound is saturated.

### 3. The Spin-SYK model

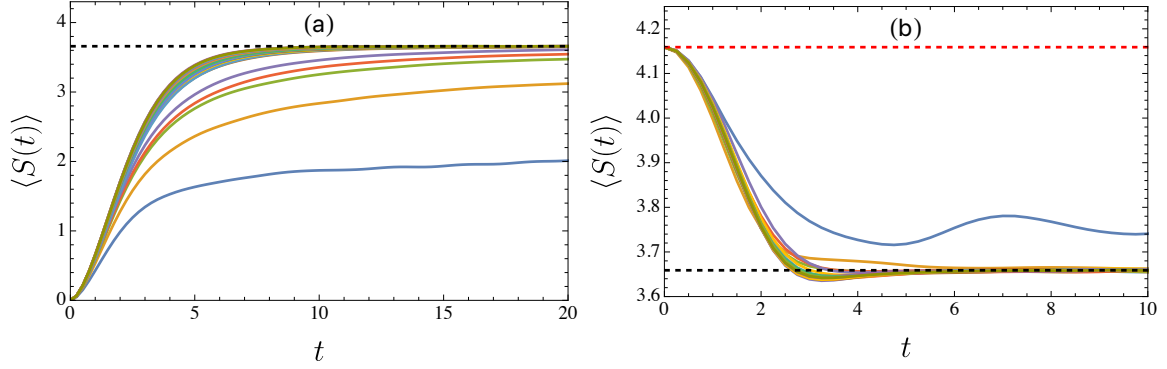


FIG. 9. (a) EE evolution of an initial product state with time, for various system fractions, for the sparse spin SYK model. The horizontal black line corresponds to the analytical result given by either Eq. (C2) or Eq. (1). We take  $N = 12$  and averaging is done over 50 realizations. We take values as  $p = 0.001, 0.002, 0.003, 0.004, 0.005, 0.01, 0.012, 0.013, 0.014, 0.015, 0.016, 0.017, 0.018, 0.019, 0.02, 0.03, 0.04, 0.05, 0.06, 0.07, 0.08, 0.1, 0.25, 0.5, 1$ . (b) EE evolution of a maximally entangled state with time, for various system fractions. The horizontal black line corresponds to the analytical result given by either Eq. (1). We take  $N = 12$  and averaging is done over 50 realizations. The critical value of  $p$  after which the entanglement entropy does not reach the theoretical bound, for initial product state, is  $p_c = 0.01$ , which is much higher as compared to SYK<sub>b</sub> and SYK model. For the case when initial state is a maximally entangled state we find  $p_c = 0.001$ , comparable to SYK model.

### 4. Autocorrelation function

We now show further supporting results for the behavior of autocorrelation function.

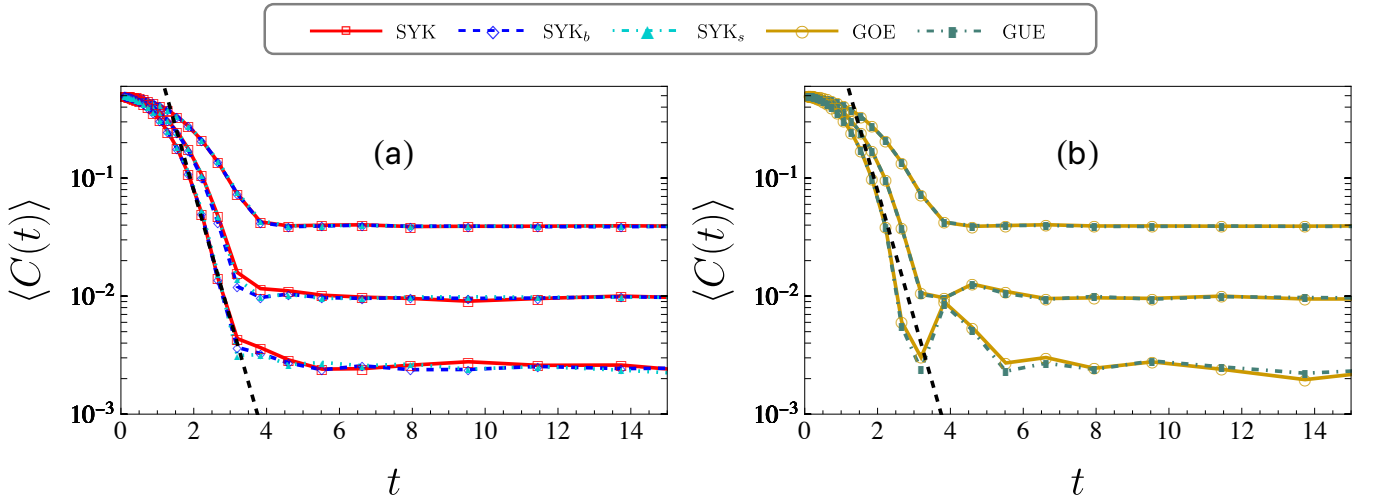


FIG. 10. (a) Autocorrelation function for Majorana operator  $\hat{O} = \psi_1$ , for different kinds of SYK model. The overlapping legends are for SYK, SYK<sub>b</sub> and SYK<sub>s</sub> for  $N = 16(10000), 24(500), 32(50)$  of Majorana fermions (and  $N/2$  number of spins for SYK<sub>s</sub>). The number in the bracket denotes the number of Hamiltonian realizations. We only consider odd parity sector. (b) Autocorrelation function for corresponding random matrices of GOE and GUE type of dimensions  $2^{N/2-1}$ . Black dashed curve represent the best fit curve;  $ae^{-bx}$ ;  $b = 2.49 \pm 0.23$ , in the exponential decay regime obtained using the data for  $2^{15}$  dimensional random matrices.

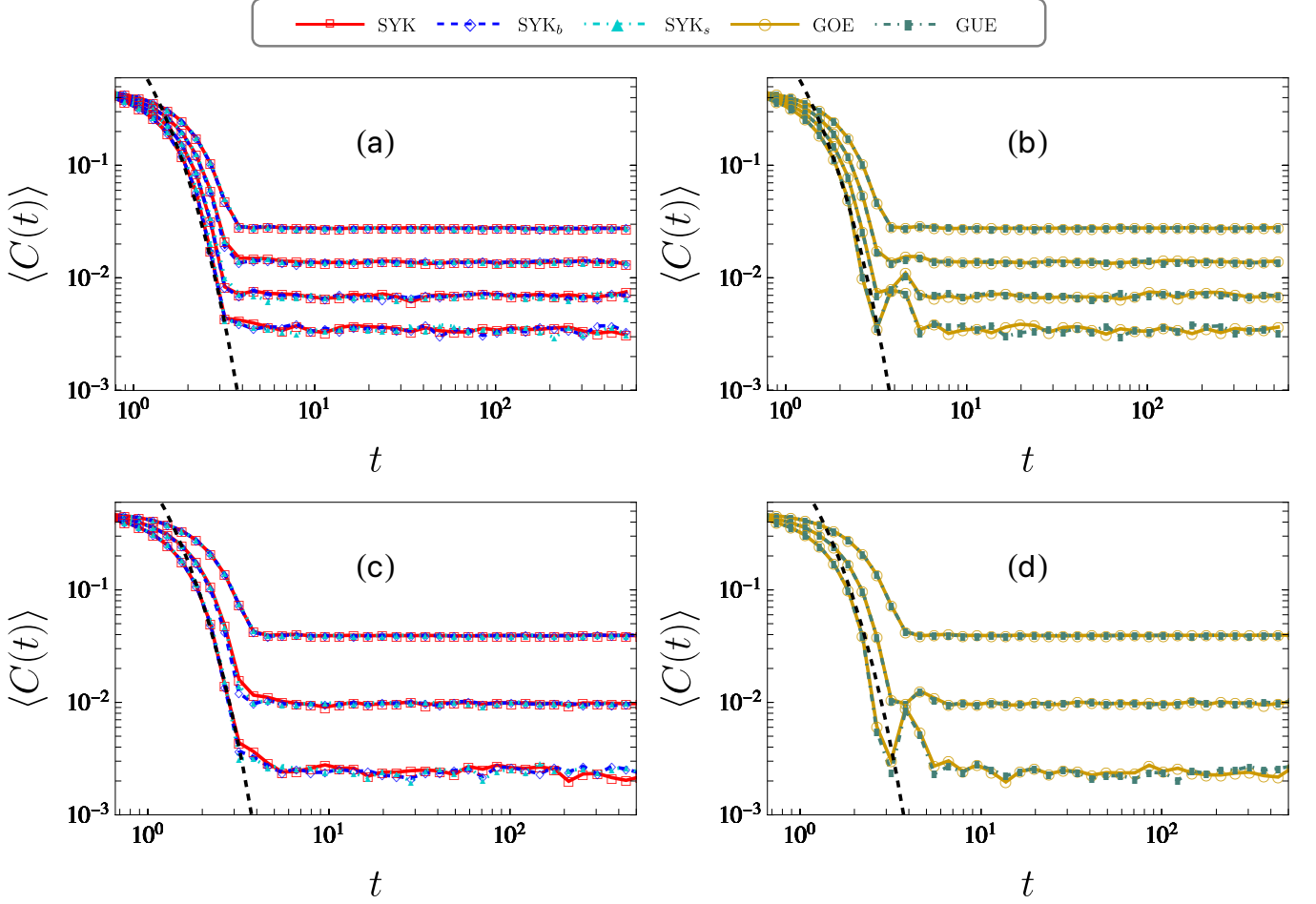


FIG. 11. (a) Late time behavior for the autocorrelation function (in a ln-ln plot) for Majorana operator  $\hat{O} = \psi_1$ , for different kinds of SYK model. The overlapping legends are for SYK,  $\text{SYK}_b$  and  $\text{SYK}_s$  for  $N = 18(5000), 22(1000), 26(200), 30(100)$  of Majorana fermions (and  $N/2$  number of spins for  $\text{SYK}_s$ ). The number in the bracket denotes the number of Hamiltonian realizations. We only consider odd parity sector. (b) Autocorrelation function for corresponding random matrices of GOE and GUE type of dimensions  $2^{N/2-1}$ . Black dashed curve represent the best fit curve;  $ae^{-bx}$ ;  $b = 2.49 \pm 0.23$ , in the exponential decay regime obtained using the data for  $2^{14}$  dimensional random matrices. (c) and (d) Same as (a) and (b) but for  $N = 16(10000), 24(500), 32(50)$  of Majorana fermions (and  $N/2$  number of spins for  $\text{SYK}_s$ ) and random matrices of dimension  $2^{N/2-1}$ .